Materials Research Proceedings 28 (2023) 2049-2060 https://doi.org/10.21741/9781644902479-220

Control strategy for angular gradations by means of the flow forming process

KERSTING Lukas[1,a], ARIAN Bahman[2,b], ROZO VASQUEZ Julian[3,c], TRÄCHTLER Ansgar[1,4,d], HOMBERG Werner[2,e] and WALTHER Frank[3,f]

[1]Fraunhofer Institute for Mechatronic Systems Design (IEM), Paderborn, Germany

[2]Paderborn University, Forming and Machining Technology (LUF), Germany

[3]TU Dortmund University, Chair of Materials Test Engineering (WPT), Germany

[4]Heinz Nixdorf Institute (HNI), Paderborn University, Germany

[a]lukas.kersting@iem.fraunhofer.de, [b]ba@luf.uni-paderborn.de, [c]julian.rozo@tu-dortmund.de, [d]ansgar.traechtler@hni.uni-paderborn.de, [e]wh@luf.uni-paderborn.de, [f]frank.walther@tu-dortmund.de

Keywords: Flow Forming, Graded Structures, Control Strategy, Closed-Loop Property Control

Abstract. Climate change, rare resources and industrial transformation processes lead to a rising demand of multi-complex lightweight forming parts, especially in aerospace and automotive sectors. In these industries, flow forming is often used to produce cylindrical forming parts by reducing the wall thickness of tubular semifinished parts, e.g. for the production of hydraulic cylinders or gear shafts. The complexity and functionality of flow forming workpieces could be significantly increased by locally graded microstructure and geometry structures. This enables customized complex hardness distributions at wear surfaces or magnetic QR codes for a unique, tamper-proof product identification. The production of those complex, 2D (axial and angular) graded forming parts currently depicts a great challenge for the process and requires new solutions and strategies. Hence, this paper proposes a novel control strategy that includes online measurements from an absolute encoder to determine the angular workpiece position. Workpieces of AISI 304L stainless steel with 2D-graded structures are successfully manufactured using this new strategy and analyzed regarding the possible accuracy and resolution of the gradation. At this point, a dependency of the gradations on the sensor and actuator dynamics, accuracy and geometry could be noted. It is further evaluated how the control strategy could be extended by an observer-based closed-loop property control approach to enhance the accuracy of the suggested strategy.

Introduction

Current developments and transformation processes like climate change, the transition to electric vehicles and the rising scarcity of resources depict a great challenge for products as well as for production processes. Especially in the automotive, aerospace and railway industry, there is therefore a rising demand for high strength, lightweight forming parts [1]. Furthermore, product counterfeiting is a serious problem in several industrial fields. A locally graded microstructure distribution on the surface of a forming part could be a feasible new solution for both cases. This could be e.g. an invisible, magnetic QR code for unique product identification against counterfeiting or a locally restricted hardness distribution at wear surfaces that allows reducing the wall thickness of the components.

To produce those customized parts, there is a need of flexible forming processes that allow individual product shapes or product features by function integration in small batches. At this point, classical die based-forming processes like deep drawing are rather at a disadvantage since the product shape is defined by the product-specific tool design. Thus, incremental forming

processes with mobile, universal tools like in the flow forming process are preferred in this case [2]. Flow forming is already used in the automotive and aerospace industry to produce cylindrical forming parts by reducing the wall thickness of tubular semifinished parts, e.g. for the production of hydraulic and pneumatic cylinders or gear shafts [3]. According to current knowledge, angular graded microstructure profiles have not yet been added to the products like an invisible QR code that represents additional functionality.

The process-integrated manufacturing of those novel graded parts requires special control strategies and information of the angular workpiece position during the whole process. For this purpose, a new control strategy is subsequently proposed in this paper that includes the sensor feedback of an absolute encoder to coordinate the actuator motion. Thus, it is possible to produce flow forming parts with locally restricted forming areas. These forming areas - in contrast to the workpiece area outside - incorporate a martensitic microstructure which is caused by deformation in terms of a strain-induced phase transformation. In the following, the special axial and angular restricted areas with a different microstructure are called 2D gradation. Each gradation produced by the proposed control strategy features a certain local accuracy which is further analyzed in this paper. Building on this, a closed-loop property control can be prospectively designed to enhance the accuracy of the gradations and simultaneously adjust geometric and material properties, so that the created QR code will be manufactured invisible.

Setup

Process and material.

This paper focusses on backward flow forming on a single roller flow forming machine. The investigations were performed with seamless tubes of stainless steel. The semifinished parts own a length of $L = 120$ mm, an outer diameter of $d_O = 80$ mm and a nominal wall thickness of $w = 4$ mm. The tubes are manufactured according DIN1127. Thus, the tubes feature an angular wall thickness eccentricity due to fabrication tolerances, with a deviation between maximum and minimum value of up to 15% [4]. The tube material is AISI 304L (X2CrNi18-9, 1.4307) which is a metastable austenitic stainless steel. By plastic deformation of this steel, a strain-induced phase transformation from austenite to α'-martensite can occur [5, 6] that influences the workpiece properties like the hardness and the micromagnetic properties. The process and material were already used in previous publications of the authors. Thus, it is referred to [7, 8] for additional information.

Machine and sensor concept.

The experiments were executed on a PLB 400 single roller spinning machine originally manufactured by Leifeld Metal Spinning GmbH (Ahlen, Germany) and later modified. The current setup is shown in Fig. 1 and was previously published in [7]. Here, the roller (entry angle $\alpha = 12°$, transition radius $R = 2$ mm, exit angle $\beta = 5°$) is mounted on a hydraulic actuated cross support that can be moved position-controlled in axial (x) and radial (y) direction for forming the workpiece. The specimen is positioned on a mandrel that is set into rotation by a spindle with an electric drive motor. The mandrel is also supported by two stationary rollers in opposite direction to the tool to compensate the high forming forces and to avoid mandrel deflection.

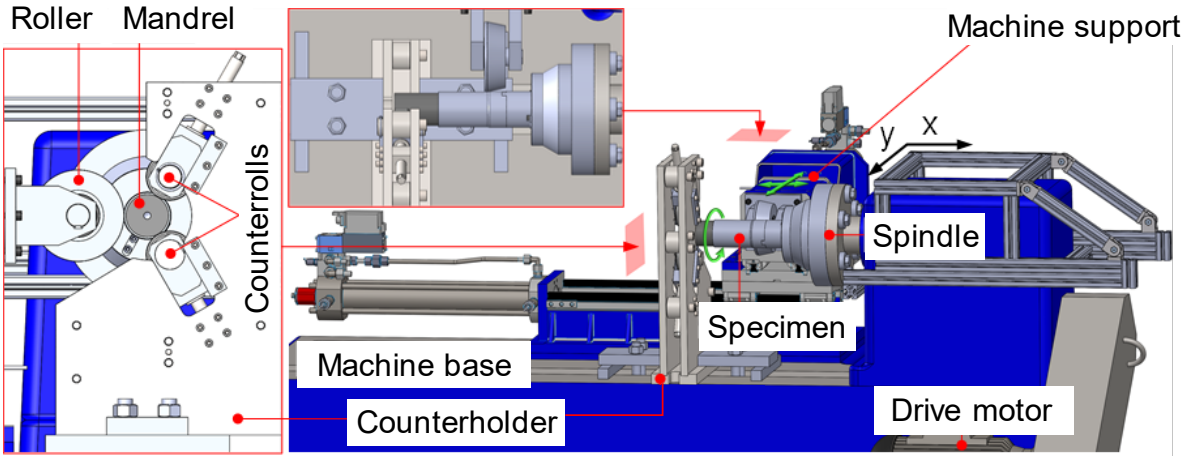

Fig. 1. Machine setup.

The machine setup includes an additional sensor system for angular gradations and property control purposes (see Fig. 2). An absolute encoder Hengstler Acuro AC58 is mounted at the end of the spindle shaft for the determination of the angular workpiece position and of the rotational speed. The sensor is specified with a resolution of 12 bit and 2048 incremental pulses in the single turn mode. The machine also contains a laser distance measuring system for measuring the resulting wall thickness reduction online during the forming process. Two laser sensors OM70 by Baumer Electric are connected to the machine support moving axially along the workpiece. One of the sensors points perpendicularly near of the forming zone with an angular offset of 90°, but no axial offset. The second sensor is positioned with an additional axial offset of 5 mm in front of the forming zone. While the first sensor is measuring the formed area, the latter measures the unformed. It is thus possible to calculate the resulting wall thickness reduction from the differential signal of both sensors. The sensor system also contains a micromagnetic 3MA-II sensor that is out of the focus of this paper (see [8] for additional information about the sensor concept).

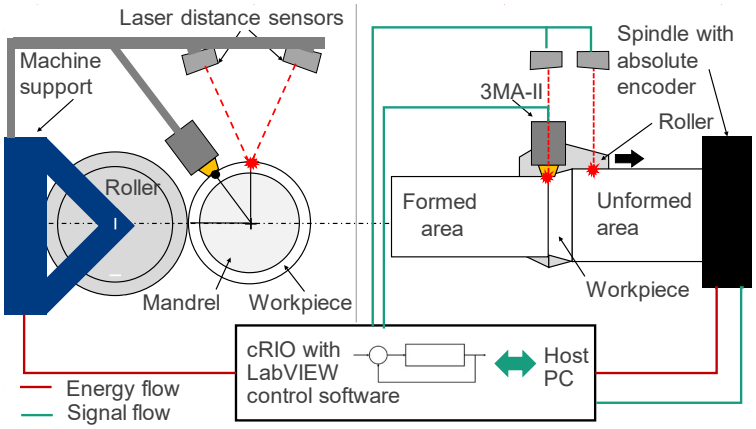

Fig. 2. Sensor concept (scheme).

Machine control architecture and control strategy.

The flow forming machine is equipped with a NI compactRIO real-time controller (cRIO 9035). On the controller, the overall machine control is executed including the position closed-loop control of the two hydraulic actuators and the control of the spindle motor. The additional sensor system is also connected to the cRIO controller (see [8] for further details). The absolute encoder transmits the measured rotational position and speed digitally using the BiSS-C protocol to a

special encoder module (SEA 9521) of the cRIO. The control on the cRIO is programmed in the LabVIEW development environment. It is a free programmable, CNC-orientated control software that was developed in [9] and [10] and extended in [8] for property control issues. In the control program, the toolpath is defined by

$$P = \begin{bmatrix} x_1 & y_1 & f_{x,1} & f_{y,1} & \theta_1 & n_1 \\ \vdots & \vdots & \vdots & \vdots & \vdots & \vdots \\ x_M & y_M & f_{x,M} & f_{y,M} & \theta_M & n_M \end{bmatrix} \quad (1)$$

Each row corresponds to a block of a conventional NC program. In each block, the desired final tool position in axial direction x and in radial direction y is defined, and in addition the feed in both directions for the tool movement (f_x and f_y) until reaching the specified final position. Those values act as an input to the internal position control of the machine support. The program is added in this paper by two additional columns for the rotational speed n and the desired angular position of the mandrel θ. Here, a transition to the next block (with new desired values for x_i, y_i, $f_{x,i}$ and $f_{y,i}$) is enforced when the measured value θ_{mes} amounts approximately θ_i. Since the absolute encoder delivers the measurement values with a certain accuracy and the rotation of the mandrel takes places continuously without stopping at θ_i, it is thus necessary to utilize a threshold value ε for defining the transition condition:

$$|\theta_{mes} - \theta_i| < \varepsilon \quad (2)$$

Procedure

Effective resolution of the absolute encoder within the control system.

For defining a suitable threshold value, the effective resolution of the absolute encoder within the setup is determined at first. It generally depends on the nominal resolution of the encoder itself and the signal sampling of the control system. For this purpose, the time signal of the absolute encoder is analyzed at different rotational speeds from 3 to 50 rpm. By comparing the measured angle values between two consecutive sample values, the effective angular resolution $\Delta\boldsymbol{\theta}$ is determined (see Fig. 3).

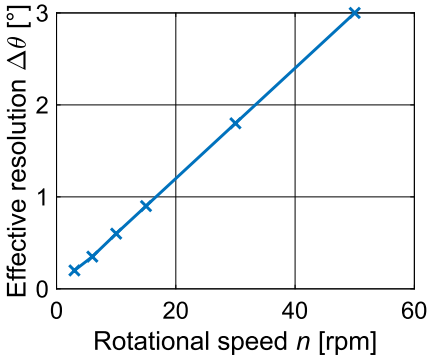

Fig. 3. Working principle of the forming control for angular parts.

The effective resolution $\Delta\theta$ significantly depends on the rotational speed n. It varies between 0.2° at the lowest speed and 3° at the highest. This effect is caused by the sampling time of the control system $t_{sample} = 0.01$ s. Since the nominal sensor resolution amounts $\Delta\theta_{nom} = \frac{360°}{2^{12}} = 0.088°$ and is much higher, the sampling effect is clearly dominating regarding the resolution. From the effective resolution, a suitable threshold value for the control can be defined since the threshold

should be greater (or equal at minimum) than the effect. In the worst case, the resolution is 3° in the experiments. Thus, the threshold value ε for the control is determined to ±3° in this paper.

Determination of the desired values (control strategy).

To produce axial and angular graded surface elements of 45°, 90° and 180° on the tube, an angle-dependent control strategy must be defined. In this paper, a rectangular strategy for the desired control values is proposed that alternates the actuator position in radial direction between a position near above the tube surface and a second position that corresponds to a desired infeed depth (see Fig. 4). The switching point of the desired value is

$$i \cdot \Delta\theta_{grad,des} \quad \text{for } i = 0 \ldots \frac{360°}{\Delta\theta_{grad,des}} \tag{3}$$

e.g. 0°, 90°, 270°, where $\Delta\theta_{grad,des}$ is the desired gradation angle. The sequence is repeated for several revolutions. Concurrently, an axial feed movement is defined. Thus, a gradation area occurs on the workpiece surface through the superposition of rotation and axial feed.

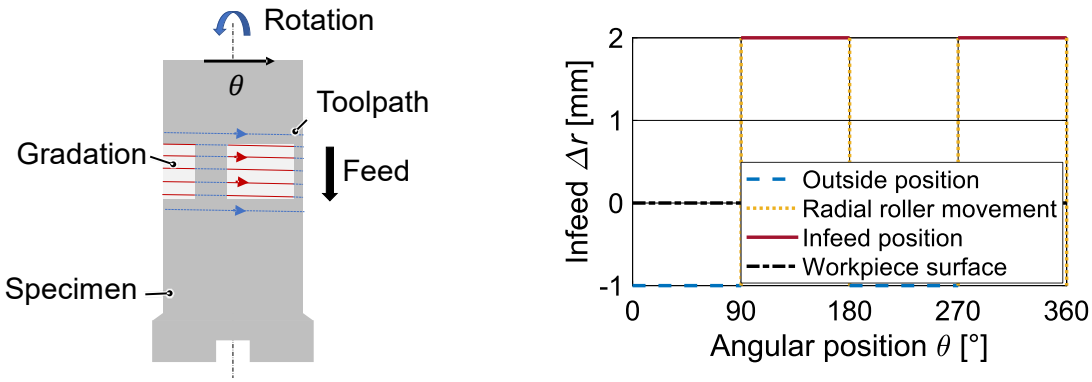

Fig. 4. Control strategy for 90°-gradations - desired actuator toolpath.

Experimental investigation by forming graded structures.

Two geometric gradation structures were investigated on specimens with the novel control strategy to validify the strategy and to analyze the accuracy of the produced gradations. Both specimens include three annular areas where gradations are placed. In the first area, a single gradation with $\Delta\theta_{grad,des} = 180°$ is placed, two 90°-gradations in the second and four 45°-gradations in the third (see Fig. 5).

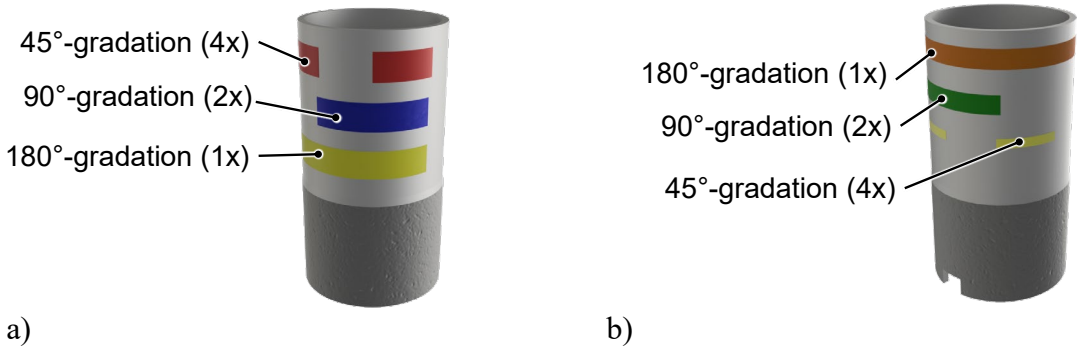

a) b)

Fig. 5. Specimen 1 (a) and specimen 2 (b) with graded structures.

Both specimens differ in the axial width of the gradations. In specimen 1, the axial width of each gradation is equal while the width is varying in specimen 2 by contrast. Here, the width is defined

by the number of rotations during the production of the specimen: 8 rotations for 180°-gradations, 4 rotations for 90°-gradations and 2 rotations for 45°-gradations. Thus, the width declines the shorter the gradation angle in this specimen.

Both experiments were performed with an axial feed of 0.1 mm/s according to former flow forming experiments of the authors in [7]. The rotational speed was defined by 5 rpm and the radial feed was set to 10 mm/s. The radial feed value f_y was determined after preliminary investigations (specimen type 3). Here, f_y was varied between 1 and 18 mm/s by a constant rotational speed of 5 rpm and a constant nominal gradation length (desired gradation angle) of 90°. This experiment was carried out without axial feed and only by performing a single rotation.

Results

Investigation on the radial feed.

At first, a specimen type 3 (produced with different radial feeds) was evaluated regarding the total length of the gradation. Since the gradations depict local areas with a reduced wall thickness and a gleaming, it was possible to evaluate the graded areas using a flexible measuring tape.

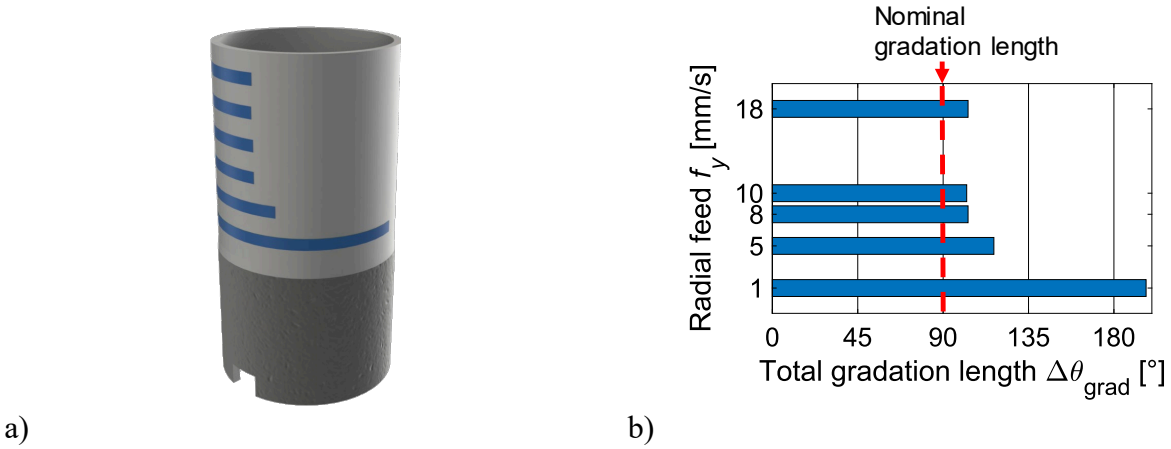

a) b)

Fig. 6. Influence of the radial feed/infeed velocity on the total angular gradation length: specimen (a) and results (b).

It can be seen from Fig. 6 that the total gradation length differs in every case from the desired nominal length of 90°, which is defined by the control. At a radial feed of 1 mm/s, the measured length amounts more than 180°. The total gradation length is significantly reduced by increasing the feed from 1 mm/s up to 8 mm/s. This is due to the shorter time the actuator takes until reaching the desired infeed position (see Fig. 8a). For infeed velocities of more than 8 mm/s, the total gradation length converges to approx. 103° despite of the faster actuator. This effect is probably caused by the contact area between roller and workpiece. Hence, the oversize of 13° cannot be compensated by a higher actuator dynamic. Additionally, a strong vibration occurs at the counter holder of the machine for radial feeds of more than 10 mm/s. The following experiments on different nominal gradation lengths are thus performed with a radial feed of 10 mm/s.

Local resolution and accuracy of the gradations.

Both specimens with different nominal gradation lengths (specimen 1 and 2) were analyzed regarding the gradation geometry and length. Hence, it is possible to exactly determine the resolution/accuracy of the gradations and to obtain a correlation between the resulting and nominal gradation length, which is the input to the control.

On specimen 2, the gradation width was also varied. Thus, there are gradations of a single rotation (single turn gradation) and of multiple rotations (multi turn gradation). A single turn gradation consists of three regions in axial and angular direction (see Fig. 7). In angular direction,

the gradation consists of three areas: a full width main area and two transition areas at the beginning and the end where the width increases or declines. Therefore, two different lengths of gradation could be distinguished: the inner length of the full width area and the total angular length of the gradation (full width area length + transition area length) that was already used as a measure in the preliminary investigation. The shape of the transition areas is mainly influenced by the roller geometry since the wall thickness is not constant in the axial direction of the whole gradation. There are two inclined surfaces in axial direction at the beginning and at the end of the gradation with a declining/increasing wall thickness. The inclined surfaces (entry and exit region) are caused by the entry and exit angle of the roller while the deepest point of the gradation corresponds to the nose region of the roller [11]. In the transition areas, the width of the entry and exit region decreases/increases to/from zero while the nose region exists on the whole length of the gradation.

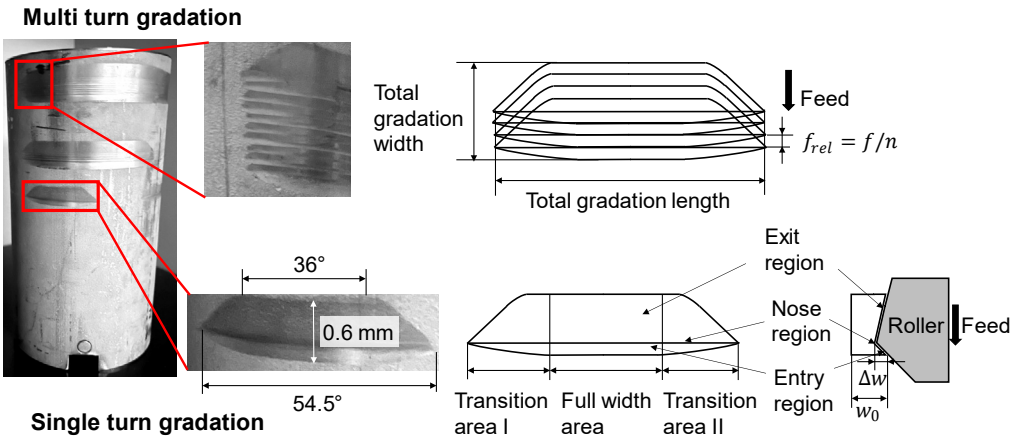

Fig. 7. Geometry of the gradations.

On the multi turn gradations (90° and 180°), the entry and exit region is rarely visible. This is due each multi turn gradation consists of a superposition of single turn gradations that are axially displaced by the related feed f_{rel} in axial direction. Through the axial feed, the entry and exit area are repeatedly shifted by the nose radius of the roller. The entry and exit region thus exist only on the two axial edges of the gradation. Hence, the full width area can only be measured at the edges while the length of the plan area inside the gradation corresponds to the total gradation length.
The results of the length measurement are summarized in Fig. 8b taking the example of specimen 2, but generally the results for specimen 1 are similar. In each case, the total angular gradation length exceeds the desired value of 45°, 90° or 180° (nominal gradation length) by approx. 15 – 25°, like in the results from the preliminary investigations. The precise value might vary between the gradations due to the accuracy of the switching condition (ε-condition, see section 2) up to ±3°. The full width area length amounts approximately 18° less than the total angular length of the gradation in every case. It can be seen that the mean value of the total angular length and the full width area length is approximately (with the accuracy of ±3°) equal to the nominal gradation length from the control. There are principally two reasons for the existence of the transition areas at the edges of the full width area: the actuator dynamics and the roller geometry. In case of the 90°-gradations, the actuator takes 2° until entering the workpiece surface and additional 7° until reaching the desired infeed of 2 mm (see Fig. 8a). Exactly 90° after starting the motion, the actuator is leaving the workpiece (with the same duration as entering but vice versa). This obviously leads to an angular displacement of the gradations of $2 \cdot 2°$ and to the elongation of the gradations due to the transition areas by $2 \cdot 9°$. Otherwise, it has been seen from the preliminary investigations that a higher actuator dynamic of more than $f_y = 10$ mm/s does not influence the total length of the gradations anymore. In this case, also the roller geometry in

circumferential direction leads to the transition area. This is due to the contact area between tube and roller that corresponds to an intersection of a cone (roller) and a cylinder (tube, see [11] for further information regarding the contact geometry).

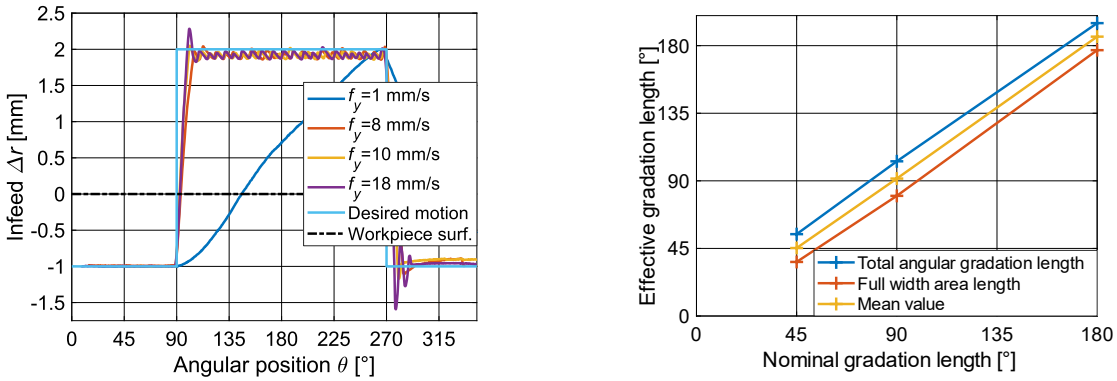

a) b)

Fig. 8. Influence of the radial feed/infeed velocity on the effective angular gradation length: a) measured actuator dynamics, b) measured gradation length.

By conclusion from the investigations on accuracy, the resulting gradation geometry is mainly influenced by the transition areas at the left and right edge of the gradation. Using the correlation from Fig. 8b, it could be possible to adjust the nominal gradation length in the control to receive a full width area length or total gradation length that matches to a desired value. But in every case, there will be a fuzziness of the gradation due to the physics of the actuator and roller geometry. In this context, also the minimal dimension of a gradation with the current machine setup (process parameter, controller, infeed, and roller geometry) can be derived. Here, the minimal angular length is 18° since the angular gradation length minimally amounts to the length of both transition areas. The minimal axial width corresponds to the width of a single turn gradation, namely the width of the entry, nose and exit region. In the experiment with an infeed of 2 mm, the minimal width amounts approximately 0.6 mm. Generally, it also depends on the wall thickness reduction since the contact area between roller and tube differs.

Wall thickness reduction of the gradations.

The gradations were also investigated regarding the resulting wall thickness reduction. Therefor, a caliper Kroeplin D4R50 (resolution: 0.05 mm) was used. The measured average wall thickness inside the gradations of specimen 1 amounts 3.74 mm, and in specimen 2 the wall thickness is 3.78 mm. The average initial wall thickness also differs between both specimens (3.95 mm for specimen 1 and 4.03 mm for specimen 2). The resulting wall thickness reduction is thus 0.21 mm (specimen 1) and 0.25 mm (specimen 2) which is nearly the same regarding the accuracy of the caliper. Hence, a deviation between the infeed of the roller (2 mm) and the thickness reduction is observed. This effect is essentially caused by undesired machine behavior, e.g. the flexibility of the support and the mandrel, and was already detected during previous investigations at the same machine (see [7] for example). The detailed results for each gradation are shown in Fig. 9. In angular direction, the wall thickness slightly differs between each gradation and moreover inside of them. This effect is caused by the eccentricity of the semifinished parts.

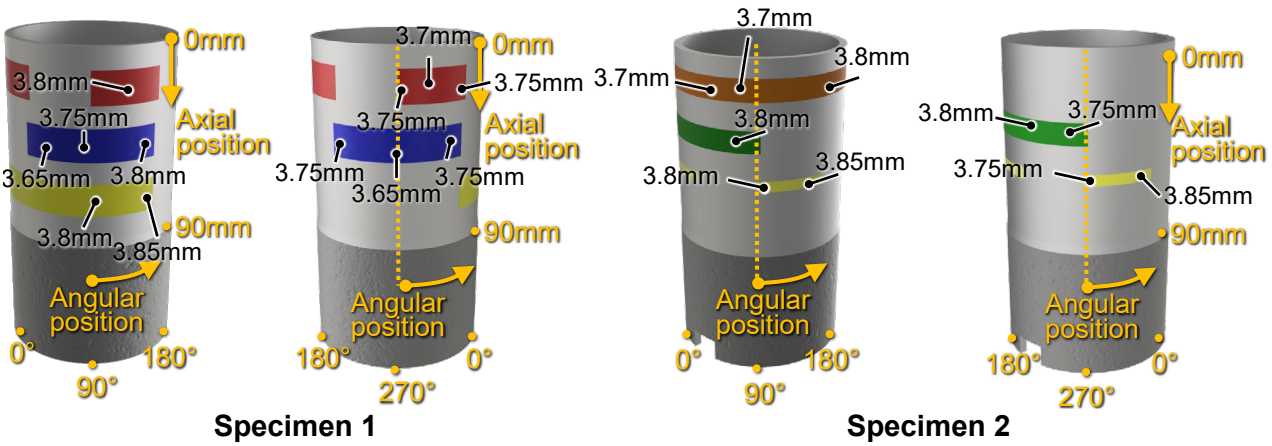

Fig. 9. Measured wall thickness inside the gradations.

α'-martensite formation inside the gradations.

A deformation-induced α'-martensite formation inside the gradations was expected due to metastable austenitic semifinished parts and the wall thickness reduction inside the gradations. For this purpose, the specimens were also analyzed by Feritscope FMP30 (Helmut Fischer GmbH, Sindelfingen, Germany) to detect the volume fraction of the α'-martensitic phase. The results (see Fig. 10) were measured at intervals of 5 mm in axial and 12° in angular direction.

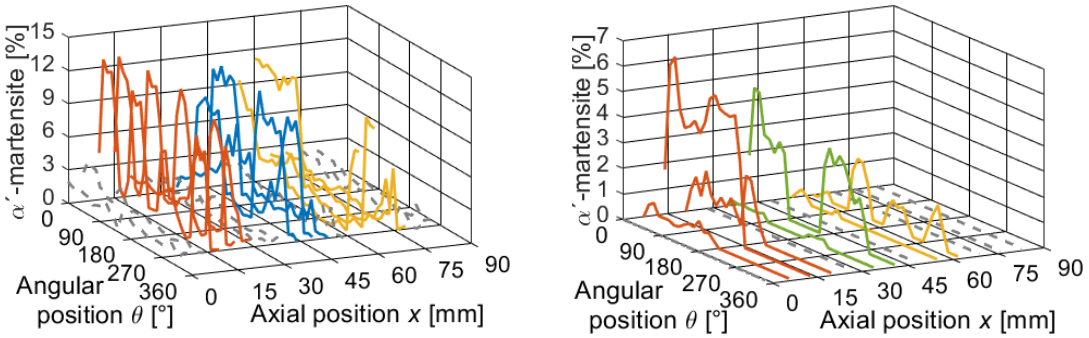

Fig. 10. Measured α'-martensite volume fraction of specimen 1 (left) and specimen 2 (right).

In each gradation of specimen 1, an α'-martensite volume fraction of approximately 11% was measured. In the non-deformed areas by contrast, the α'-martensite amounts less than 3%. Thus, a clearly graded α'-martensitic structure could be identified. On the axial edge of each gradation, the peak value of the α'-martensite measurement is on a lower level (e.g. 5% for the 90°-gradations). This effect could be influenced by the sensor spot that measures inside and outside the gradation at the edge. In angular direction, there is also a gradient of the measured amount of α'-martensite. At the beginning of the gradation (inside transition area I), the α'-martensite amount is lower than at the middle (full width area), where a maximum is reached, and decreases again until the gradation end (transition area II). This is because the contact conditions between tool and workpiece are optimal at the center. However, while forming the gradations, a forming force gradient is created over the material until the optimal contact conditions are reached (at the beginning) or released (at the end), which is reflected in the angular α'-martensite gradient.

Online measurements of the wall thickness reduction during forming.

Regarding a future use in a property control for 2D gradations, the measurements of the two laser distance sensors were also recorded during the production of the two specimens. Sensor 1 was placed on the same axial position as the forming tool, but with an angular displacement. Here,

the distances between the two sensors and the workpiece arise when the support starts infeeding at $t = 98.5$ s/$\varphi = 182°$ (see Fig. 11). Similarly, the distances decline with a distinct downshift at $t = 104.9$ s/$\varphi = 360°$ while the support moves back into the starting position. Both distance shifts are similar, so no wall thickness reduction is detected during the support motion. Wall thickness reduction is firstly measured with a temporal delay of 3.3 s to the actuator signal starting at $t = 101.8$ s/$\varphi = 275°$ and ending at $t = 108.2$ s/$\varphi = 90.5°$. This temporal delay is caused by the angular displacement between sensor and forming zone that amounts approximately 90°. The signal difference of both laser distance sensors amounts approximately 0.3 mm which corresponds roughly to the manually measured wall thickness reduction values.

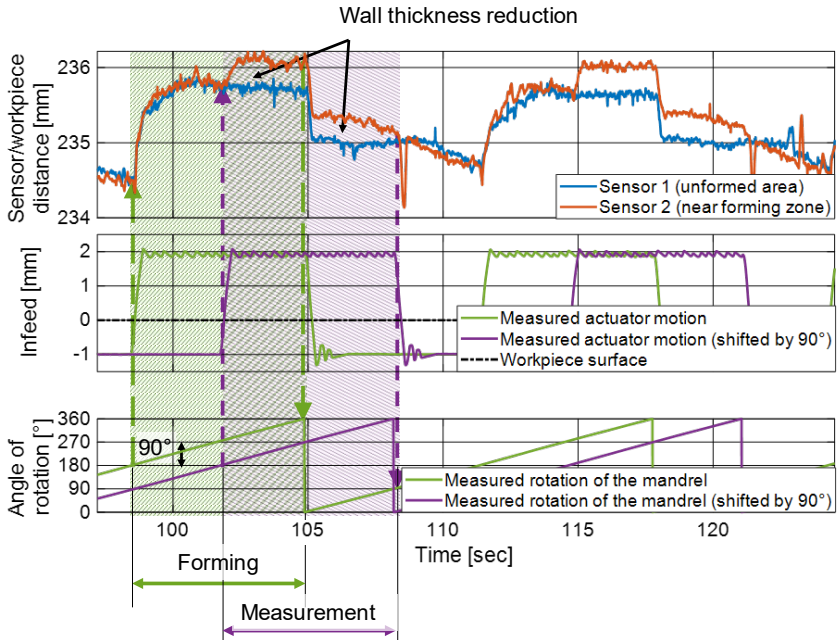

Fig. 11. Influence of the actuator movement and angular sensor displacement on the online wall thickness measurement (forming and measurement of the gradation).

Summary

In this paper, a novel control strategy for the flow forming process was presented. Here, flow forming was enabled to more complex, 2D (axial and angular) graded structures on the specimen surface like a QR code by integrating an absolute encoder into the control. This encoder-based control strategy was successfully validated by the experimental manufacturing of locally graded forming parts. The resolution and accuracy of these gradations in angular direction significantly depend on the actuator dynamics, namely the infeed velocity/feed in radial direction. Above a certain critical velocity, the effect of the actuator dynamic decreases. In this case, the imprint of the roller geometry on the specimen (contact area) becomes the dominating effect. The result is that the gradations own a greater total angular length than the actuator feeds in. In axial direction, the gradation edges were also influenced by the roller geometry. For this reason, a minimal gradation dimension of 0.6 mm in axial and of 18° in angular direction was concluded from the experiments. Thus, a required line thickness of 0.5 to 4 mm for a QR code could be almost realized. In angular direction, structures of 4° to 40° were required since multiple gradations should be circumferentially placed for a QR code. For this purpose, different roller geometries will be evaluated in further investigation to enhance the accuracy due a dependence on the roller radius is assumed. Besides the dimensional accuracy in angular and axial direction, the specimens were also investigated regarding the wall thickness reduction in radial direction. Here, a significant deviation between infeed and thickness reduction was noticed. Nevertheless, the wall thickness reduction

also leads to an α'-martensite formation and thus to a locally graded α'-martensite structure on the specimen. The resulting magnetic properties of the α'-martensite structure will be analyzed in future research.

The presented control strategy could be further extended by a closed-loop control of the wall thickness reduction to compensate the deviation of the reduction. Concurrently, it would be favorable to adjust the α'-martensite volume fraction by a closed-loop property control to a defined value (see Fig. 12).

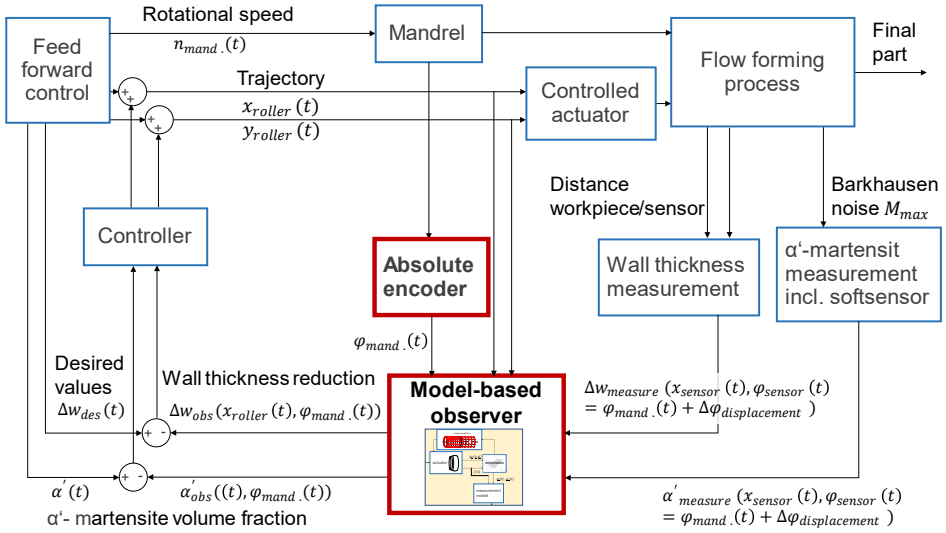

Fig. 12. Concept of a closed-loop property control structure with a model-based observer.

As seen from the measurements of the laser distance sensors, such a closed-loop control for 2D gradations is difficult since the forming result is detected with a spatial and temporal displacement. Therefore, it is not possible to simply compare the measured value to the desired. A possible solution to overcome this challenge is to include a model-based observer into the closed-loop control structure (see Fig. 12). The observer could allocate the measured values to the correct location within a model of the specimen surface and output the wall thickness and the α'-martensite fraction at the actual actuator position. Thus, it would be possible to correctly determine the control error and enhance the process accuracy by applying a closed-loop property control to the process.

Acknowledgement

The authors would like to thank the German Research Foundation (Deutsche Forschungsgemeinschaft, DFG) for their support of the depicted research within the priority program SPP 2183 "Property-controlled metal forming processes", through project no. 424335026 "Property control during spinning of metastable austenites".

References

[1] E. Tekkaya, N. Ben Khalifa, G. Grzancic, R. Hölker, Forming of lightweight metal components: need of new technologies, Procedia Eng. 81 (2014) 28-37. https://doi.org/10.1016/j.proeng.2014.09.125

[2] D. Yang, M. Bambach, J. Cao, J. Duflou, P. Groche, T. Kuboki, A. Sterzing, A. Tekkaya, C. Lee, Flexibility in metal forming, CIRP Annals 67 (2018) 743-765. https://doi.org/10.1016/j.cirp.2018.05.004

[3] P. Groche, Flow forming, in: The International Academy for Production Engineering et al. (eds.), CIRP Encyclopedia of Production Engineering, Springer, Berlin, Heidelberg, 2019. https://doi.org/10.1007/978-3-662-53120-4

[4] DIN Deutsches Institut für Normung (ed.), Nichtrostende Stahlrohre - Maße, Grenzabmaße und längenbezogene Masse, Beuth, Berlin, 1996.
[5] J. Talonen, P. Apegren, H. Hänninen, Comparison of different methods for measuring strain induced α-martensite content in austenitic steels, Mater. Sci. Technol. 20 (2004) 1506-1512. https://doi.org/10.1179/026708304X4367
[6] P. Haušild, V. Davydov, J. Drahokoupil, M. Landa, P. Pilvin, Characterization of strain-induced martensitic transformation in a metastable austenitic stainless steel, Mater. Des. 31 (2010) 1821-1827. https://doi.org/10.1016/j.matdes.2009.11.008.
[7] B. Arian, W. Homberg, L. Kersting, A. Trächtler, J. Rozo Vasquez, F. Walther, Produktkennzeichnung durch lokal definierte Einstellung von ferromagnetischen Eigenschaften beim Drückwalzen von metastabilen Stahlwerkstoffen, in: G. Hirt (Ed.), 36. Aachener Stahlkolloquium - Umformtechnik “Ideen Form geben“, Aachen, 2022, pp. 333-347.
[8] L. Kersting, B. Arian. J. Rozo Vasquez, A. Trächtler, W. Homberg, F. Walther, Innovative online measurement and modelling approach for property-controlled flow forming processes, Key Eng. Mater. 926 (2022) 862-874. https://doi.org/10.4028/p-yp2hj3
[9] D. Hornjak, Grundlegende Untersuchungen der Prozess- und Werkzeugparameter und ihre Wechselwirkungen für das thermo-mechanisch unterstützte inkrementelle Umformverfahren des Reib-Drückens, Doctoral Dissertation, Paderborn University, Shaker, Aachen, 2013.
[10] B. Lossen, Ein Beitrag zur Herstellung von hybriden Bauteilen mittels Reibdrücken, Doctoral Dissertation, Paderborn University, Shaker, Düren, 2019.
[11] M.J. Roy, D.M. Maijer, R.J. Klassen, J.T. Wood, E. Schost, Analytical solution of the tooling/workpiece contact interface shape during a flow forming operation, J. Mater. Process. Technol. 210 (2010) 1976-1985. https://doi.org/10.1016/j.jmatprotec.2010.07.011